MABS
2021, VOL. 13, NO. 1, e1981806 (14 pages)
https://doi.org/10.1080/19420862.2021.1981806

Taylor & Francis
Taylor & Francis Group

REPORT

OPEN ACCESS Check for updates

Identification of a CE-SDS shoulder peak as disulfide-linked fragments from common C_H2 cleavages in IgGs and IgG-like bispecific antibodies

Mingyan Cao[a], Yang Jiao[a], Conner Parthemore[a], Samuel Korman[a], Jiao Ma[a], Alan Hunter[b], Greg Kilby[a], and Xiaoyu Chen[a]

[a]Analytical Sciences, Biopharmaceutical Development, Biopharmaceuticals R&D, AstraZeneca, Gaithersburg, MD, USA; [b]Purification Process Sciences, Biopharmaceutical Development, Biopharmaceuticals R&D, AstraZeneca, Gaithersburg, MD, USA

ABSTRACT

Fragmentation is a well-characterized degradation pathway of therapeutic antibodies and is usually monitored by capillary electrophoresis–sodium dodecyl sulfate (CE-SDS). Although fragments due to cleavage in C_H2 domains linked by intrachain disulfide bonds are common and can be detected by reduced reversed-phase – liquid chromatography mass spectrometry (RP-LCMS) and reduced CE-SDS methods, their separation in nonreduced CE-SDS (nrCE-SDS) has not been reported but speculated as comigrating with intact IgG. A shoulder peak in nrCE-SDS was observed in the stability samples of an IgG-like bispecific antibody and was determined to be mainly caused by fragments from clipping at the C-terminus of leucine (L)306 or L309 (EU numbering) in the C_H2 domain of both heavy chains (HCs) and, to a lesser degree, at the C-terminus of L182 in the C_H1 domain of the knob HC. Subunit LCMS analysis verified that the crystallizable fragment contained variants with one or multiple mass additions of ~18 Da due to clipping. Further investigation revealed that C_H2 clippings at L306 and L309 were largely due to proteolytic activity, and cleavages were present at various levels in all in-house IgG1 and IgG4 molecules studied. Our study shows that C_H2 domain cleavages, with complementary fragments still linked by intrachain disulfide, can be electrophoretically resolved as a front shoulder of the main peak in nrCE-SDS. Given the high occurrence of C_H2 cleavages in antibodies, these findings will have broad applicability and could help manufacturers of therapeutic antibodies in process improvement, product characterization, investigations, formulation stability, and stability comparability studies.

ARTICLE HISTORY
Received 20 June 2021
Revised 1 September 2021
Accepted 14 September 2021

KEYWORDS
IgG-like bispecific antibodies; monoclonal antibody; fragments; CE-SDS; hydrophobic interaction chromatography; intrachain disulfide bond; subunit; peptide mapping; protease inhibitor

Introduction

Fragmentation of therapeutic proteins is a critical quality attribute that is monitored to ensure product purity and integrity. Fragments can be generated during production in the cell culture and purification process and may also accumulate during storage or under stress conditions.

Size-exclusion chromatography (SEC) provides information about monoclonal antibody (mAb) aggregates as well as fragments. Although typically providing reliable quantitation for aggregates, SEC usually underestimates fragments because it often detects cleavages only in the hinge region.[1] Cleavages within the antibody folded domains (V_L, C_L, V_H, C_H1, C_H2, C_H3) held by noncovalent interactions are not readily detected by SEC.[2] These fragments are usually present in the SEC monomer and aggregate peaks. Additionally, the separation between the large hinge fragment and the SEC monomer peak is usually poor, especially for only mildly degraded samples.

In contrast, capillary electrophoresis–sodium dodecyl sulfate (CE-SDS) methods are better suited for fragment quantitation at all stages of pharmaceutical development for lot release, stability, in-process testing, characterization, and investigations.[3–11] Owing to difficulties in direct fraction collection or online coupling to a mass spectrometer, studies on CE-SDS peak identification largely rely on: 1) prior knowledge of possible species under certain conditions; 2) sodium dodecyl sulfate–polyacrylamide gel electrophoreses (SDS-PAGE) separation, gel band excision, and in-gel digestion peptide mapping; 3) gel-free fractionation, intact mass, and peptide mapping;[12] 4) SEC-based fractionation with offline intact mass, peptide mapping, and CE-SDS;[10,13,14] and 5) reversed-phase liquid chromatography (RPLC) based fractionation, intact mass, top-down tandem mass spectrometry (MS/MS), or offline peptide mapping and CE-SDS.[15]

Kubota et al.[12] used three of these approaches (in-gel digestion, RPLC fractionation, and gel-free fractionation) to investigate an unknown 10-kDa fragment and a concomitant shoulder of the monomer peak in nonreduced CE-SDS (nrCE-SDS) of a heat-stressed mAb. They determined that cleavage in the heavy-chain (HC) complementarity-determining region (CDR) 3 between arginine (R)104 and aspartic acid (D)105 led to the two new peaks, namely, the 10-kDa fragment peak and the complementary 138-kDa shoulder peak in CE-SDS of the stressed samples. In-gel digestion confirmed the N- and C-terminus of HC105-445 fragments, but the C-terminus of the 10-kDa fragment and many other peptides were not detected, possibly due to poor recovery from the gel bands or because the selectivity of the nano-column was not as broad as

CONTACT Mingyan Cao mingyan.x.cao@gsk.com Large Molecule Analytical Development, Strategic External Development, GlaxoSmithKline, 1000 Winter Street, Waltham, MA 02451, USA
Supplemental data for this article can be accessed on the publisher's website.

© 2021 Taylor & Francis Group, LLC
This is an Open Access article distributed under the terms of the Creative Commons Attribution-NonCommercial License (http://creativecommons.org/licenses/by-nc/4.0/), which permits unrestricted non-commercial use, distribution, and reproduction in any medium, provided the original work is properly cited.

that of analytical-scale columns. RPLC fractionation allowed identification of the 10-kDa fragment, which cannot be done by in-gel digestion alone due to the enzymatic treatment of the sample. The gel-free fractionation approach determined the 10-kDa fragment (HC1-104) and the complementary fragment (HC105-446) in the reduced off-gel fractions. When using this technique, however, extensive optimization of fractionation is needed to resolve closely eluting peaks observed in CE-SDS. Additionally, collecting enough material for liquid chromatography–mass spectrometry (LCMS) analysis by gel-free electrophoresis is very labor intensive.

SEC fractionation followed by CE-SDS and LCMS analysis has been used to assign hinge fragments observed in CE-SDS.[10,13] For an immunoglobulin G1 (IgG1) HC CDR fragment to present as a shoulder peak in CE-SDS, a denaturing SEC method is required to enrich the fragment for LCMS identification due to the noncovalent binding of this fragment with monomer and aggregates.[13] As in the denaturing SEC approach, after incubation at 40°C in pH 4 buffer for 12 h, an IgG1 C_H2 domain fragment resulting from concurrent cleavages on both HCs between glycine (G)240 and G241 can be detected and fractionated by SEC.[10] Two elevated CE-SDS peaks for an IgG1 incubated with iron and histidine were identified as a free light chain (LC) and an HC hinge fragment via offline LCMS analysis of the SEC fragment peak.[4] A nonreducible species observed in reduced CE-SDS (rCE-SDS) was enriched in an early eluting peak (prior to the HC peak) in reduced SEC and was identified by subsequent intact LCMS and peptide mapping as a thioether linkage between the LC and the HC.[16] In summary, SEC fractionation has been predominantly used for identification of hinge fragments in mAb therapeutics. Applications of SEC to enrich other size variants for CE-SDS peak identification are very limited and often require denaturing or reducing conditions to resolve cleaved fragments by disrupting their noncovalent bindings to monomer or aggregates in SEC.

Recently, Wang et al.[15] reported a comprehensive CE-SDS peak assignment for an IgG1 mAb. All peaks observed in both nrCE-SDS and rCE-SDS of an IgG1, with and without heat stress (40°C for 3 months), were identified through RPLC fractionation, intact LCMS, and top-down MS/MS. The CE-SDS peak assignment of cleavages in the hinge, the lower hinge/C_H2 interface and C_H2 domain and the C_H1, V_L, C_H3 determined in the study should be, in principle, applicable to similar IgG1s. Clipping within the C_H2 domain, such as the DP (aspartic acid, proline) clipping at D270 (EU numbering), is commonly observed in mAbs, even in unstressed material, as reported in this and many other studies.[2,8,11,15,17,18] C_H2 cleavages at D270, histidine (H)285, asparagine (N)286, N297, and N315 were detected only by rCE-SDS in this study. Because cleavages at these sites generate fragments that are still linked by the cysteine (C)261-C321 intrachain disulfide bond within the C_H2 domain, the authors hypothesized that these clipped, but not dissociated, species would comigrate with intact IgG in nrCE-SDS. IgGs with clipping at these sites would also tend to coelute with the intact monomer in RP-LC and hence would not be enriched in any of the RPLC fractions used for identification of size variants.

Here, we report the identification of an nrCE-SDS shoulder peak that appeared in a bispecific antibody-A (bsAb-A) sample that had been heat stressed at 40°C. Structural characterization studies revealed that the shoulder peak consisted of C_H2 and C_H1 cleavages on multiple sites with dominant cleavage sites at leucine (L)306 and L309 in C_H2. The C_H2 fragments were all still linked by the C261-C321 intrachain disulfide bond. In contrast to a previous hypothesis that the C_H2 clipped but disulfide-linked species comigrate with intact IgG in nrCE-SDS,[15] we found these species were partially resolved and migrated slightly earlier than intact IgG. When accumulated to a level sufficient to be observable by the nrCE-SDS method, these species formed a front shoulder on the main peak.

Results

CE-SDS shoulder peak from samples heat stressed at 40°C

bsAb-A is an asymmetric, IgG-like bsAb that is currently under clinical development. In a heat stress study, three bsAb-A drug substance lots, each produced at a different manufacturing site, were incubated at 40°C for up to 3 months. nrCE-SDS and rCE-SDS profiles of 40°C 3-month degraded material and degradation rates are illustrated in Figure 1. Overall profiles and degradation rates of these three manufacturing lots assessed by nrCE-SDS and rCE-SDS were deemed comparable. However, a noticeable difference in the levels of the monomer shoulder peak in nrCE-SDS was observed (Figure 1(a)): lot C, manufactured at the latest site, had the least amount of shoulder peak; lot A had the largest amount of shoulder peak; and lot B, from the earliest site, had a shoulder peak at a level between the other two lots. In rCE-SDS (Figure 1(b)), differences were observed in two peaks (indicated by red arrows) that showed trending in relative quantitation similar to that observed in the nrCE-SDS shoulder peak among the three lots. Efforts were made to identify the shoulder peak to elucidate potentially novel degradation pathways and understand its root cause, thereby potentially aiding improvements to the control of final product quality.

CE-SDS peak identification by HIC fractionation and partial reduction study

For CE-SDS peak identification, bsAb-A drug substance that had been heat stressed at 40°C for 1 month was fractionated by hydrophobic interaction chromatography (HIC) to isolate size variants. Each fraction collected was subsequently analyzed by CE-SDS (Figure 2), reversed-phase LCMS (RP-LCMS) (Supplementary Figure S1), and peptide mapping (data not shown). Correlations of CE-SDS profiles of HIC fractions with corresponding RP-LCMS data enabled us to identify the size variant peaks observed in the CE-SDS profiles (Figure 2), which were labeled from 1 to 11, with the exception of heavy-heavy-light chain (HHL) species (peak 10). HHL species in CE-SDS were identified by partial reduction for HHL enrichment and subsequent CE-SDS and RP-LCMS analysis for identification (Supplementary Figure S2). CE-SDS peak identities based on HIC fractionation and partial reduction study are listed in Table 1, and their identifications are provided in the Supplementary Material accompanying Supplementary Figures S1 and S2. With all peaks in the CE-SDS profile of the HIC fractions identified

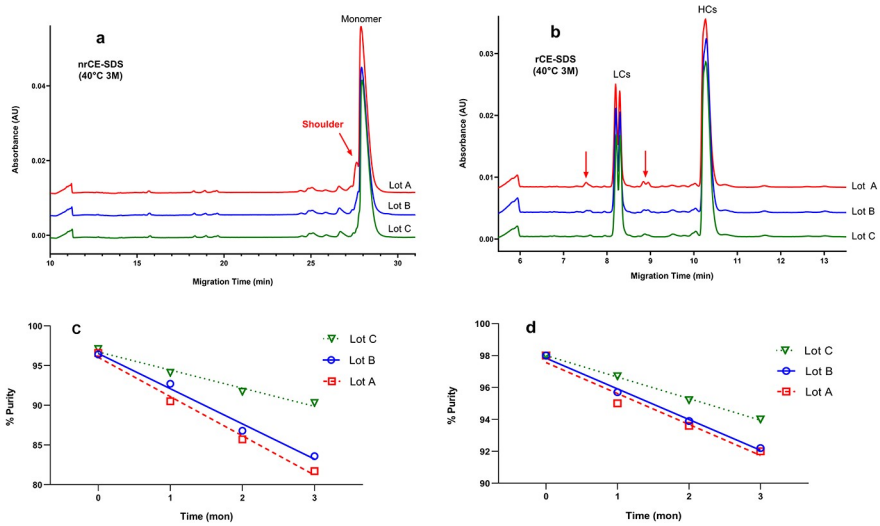

Figure 1. Comparison of nrCE-SDS and rCE-SDS profiles and degradation rates of three bsAb-A drug substance lots under stress conditions at 40°C up to 3 months. (a) nrCE-SDS overlay of heat-stressed lots A, B, and C; (b) rCE-SDS overlay of heat-stressed lots A, B, and lot C; (c) percent purity of lots A, B, and C by nrCE-SDS; (d) percent purity of lots A, B, and C by rCE-SDS.

by LCMS, we were able to label the peaks in the CE-SDS profiles of the nonstressed control and the samples that were heat stressed at 40°C for 1, 2, and 3 months (Figure 3), and correlate the N-terminal fragments with their respective C-terminal complementary fragments (Figure 3(a)). Because the CE-SDS shoulder peak was not enriched in any of the HIC fractions, its identity in the heat-stressed samples remained unknown. However, the identification of all other peaks greatly facilitated the identification of the shoulder peak in CE-SDS profiles.

Fragments in the heat-stressed samples shown in Figure 3 can be divided into two categories: 1) fragments affected only by cell culture conditions and hence unchanged in stability, and 2) stability-indicating fragments. CE-SDS peaks 3, 3′, 7, and 10 belong to category 1 and were identified as free LC (cysteine capped), light-heavy-light chain (LHL) mispair,[19] and partially reduced subunit HHL, respectively. Their intensities were almost unchanged between the control and the samples stressed at 40°C for 1, 2, or 3 months, and the LHL mispair species had no observed paired complementary fragments. In contrast, CE-SDS peaks 1, 1′, 2, 4, 5, 6, 8, 8′, 9, and 11 were formed from degraded bsAb-A and belonged to category 2 fragments. Their peak identifications are shown in Table 1. These fragments increased under stress conditions.

The unknown shoulder peak was also determined to be a stability-indicating fragment, as it increased under heat-stressed conditions (Figure 3(b)). However, unlike other stability-indicating fragments, no complementary fragment of the shoulder peak was found in the nrCE-SDS profiles of the heat-stressed samples (Figure 3(a)); fragments smaller than hole HC 1–102 (CE-SDS peak 1) were not observed in the HIC fractions or the stability samples by CE-SDS (Figure 2(a,b)) or the RP-LCMS method (Supplementary Figure S1).

In a previous study, the CE-SDS shoulder peak was identified and reported as IgG missing HC N-terminal 1–104.[12] In that report, a ~10-kDa HC N-terminal fragment (HC 1–104) was linked to the shoulder peak (IgG missing HC 1–104) by nrCE-SDS. With rCE-SDS, the 10-kDa fragment peak remained unchanged, and the complementary C-terminal fragment, HC 105–449, migrated close to HC. In this study, similar fragments due to IgG missing HC N-terminal ~100 amino acids from the hole or knob HC were also identified as peak 11 by CE-SDS of bsAb-A, and the respective ~10-kDa HC N-terminal fragments were identified as peak 1 (if cleaved from hole HC) or 1′ (if cleaved from knob HC). However, the unknown shoulder peak migrated later than peak 11, indicating a larger molecular mass than peak 11. This shoulder peak is unique in several ways: 1) it is stability-indicating but has no complementary fragment peak in nrCE-SDS (Figures 1(a) and 3(a)); 2) in rCE-SDS, two instead of one emerging HC fragment peaks were observed; and 3) trending in the intensities of the two HC fragments in rCE-SDS among the three lots was consistent with that of the nrCE-SDS shoulder peaks (Figure 1(b)), indicating that the shoulder peak potentially comprises two separate species. Hence, we hypothesized that the shoulder peak may contain fragments that have been cleaved, but are still linked by intrachain disulfide bonds. This type of fragment increases in stability but contains no complementary fragments, as fragments are still linked by an intrachain disulfide bond. However, in rCE-SDS, two increasing HC complementary fragments would be observed. Further characterization work was undertaken to confirm this hypothesis, as described below.

Identification of intrachain disulfide-linked fragments by reduced LCMS analysis and peptide mapping

Stability samples that had been stressed at 40°C for 3 months and analyzed by intact mass with and without deglycosylation, as well as subunit analysis after digestion with IgG-degrading enzyme of *Streptococcus suis* (IgdE) (FabALACTICA), showed no discernible differences between the three bsAb-A lots that could be related to the

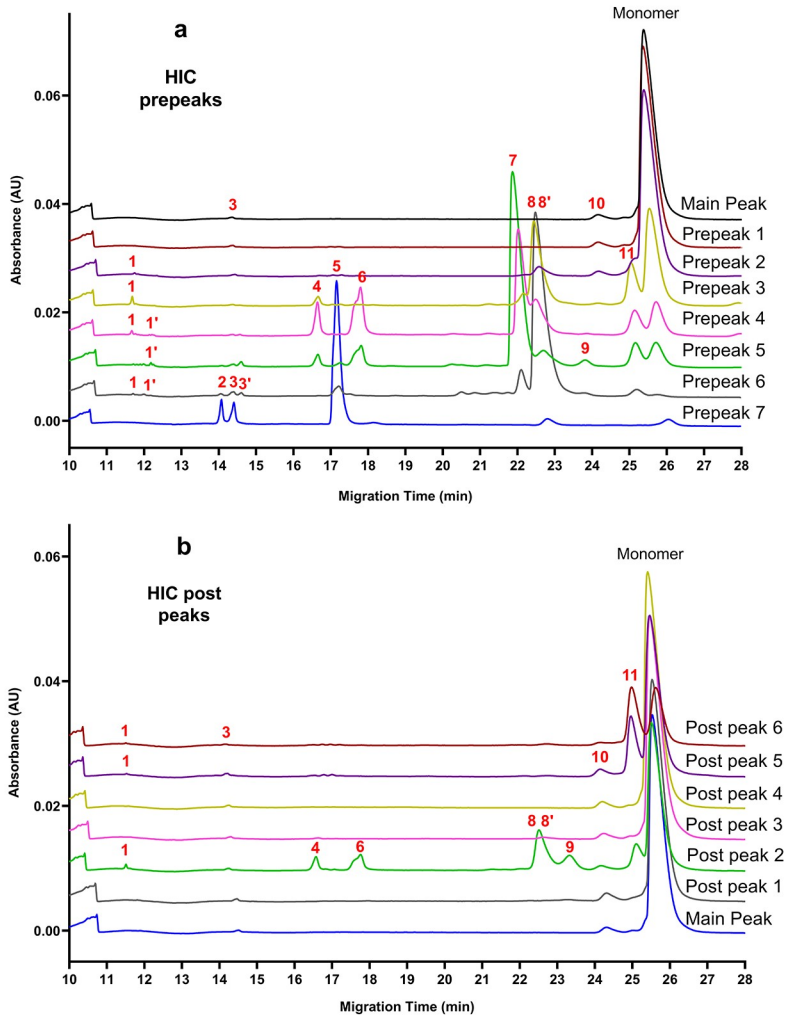

Figure 2. nrCE-SDS profiles of HIC fractions from bsAb-A drug substance that was heat stressed at 40°C for 1 month. CE-SDS size variant peaks are labeled from 1 to 11. (a) nrCE-SDS profiles of HIC pre-peaks and main peak; (b) nrCE-SDS profiles of HIC post-peaks.

unknown CE-SDS shoulder peak (data not shown). However, differences were observed in the reduced LCMS analysis, where samples were denatured and reduced in 4 M guanidine hydrochloride and 10 mM dithiothreitol to ensure that intrachain disulfide bonds were fully reduced. The resulting RPLC ultraviolet (UV) chromatograms are shown in Figure 4. Differences observed among the three lots can be attributed to C_H2 cleavages at L306, L309 on both HCs (peaks 1 and 3 and their oxidized forms; Figure 4) and C_H1 cleavage on knob HC at L182 (peak 5; Figure 4). The order of magnitude of these three cleavages in the three lots were lot A > lot B > lot C, consistent with the trend observed in the nrCE-SDS shoulder peak. C_H2 cleavage at D270 (DP clipping) is also observed at both HCs (peaks 2 and 4; Figure 4). However, unlike peaks 1, 3, and 5, the DP clipping in C_H2 (peaks 2 and 4) was comparable for the three lots. C_H2 and C_H1 cleavages detected here (peaks 1 to 5) all resulted in fragments linked by intrachain disulfide bonds. Their clipping sites, along with the deconvoluted mass spectra of the C-terminal fragments from these cleavages, are indicated in the insert in Figure 4. The complementary N-terminal fragments from these clippings were not detected, possibly due to the coelution of these fragments with other abundant species in reduced RP-LCMS analysis.

Tryptic digest peptide mapping and LCMS analysis confirmed the presence of all four of the above C_H2 fragments (peaks 1–4; Figure 4) and the C_H1 fragment (peak 5; Figure 4) in these samples. Figure 5 shows the MS/MS analysis of tryptic peptide (L)TVLHQDWLNGK and (L)HQDWLNGK resulting from C_H2 clipping at C-terminal L306 and C-terminal L309, respectively. In addition, cleavages at the amino acid sites adjacent to L306 and L309 at attenuated levels were also identified by peptide mapping; selected tandem mass spectra from cleavages at these neighboring sites are included in Supplementary Figure S3.

Table 1. nrCE-SDS peak assignment based on HIC fractionation study and partial reduction study (for peak 10 assignment).

nrCE-SDS peak no.	Fragment	Mass (Da) Theo	Mass (Da) Detect	HIC enrichment	Complementary fragment	CE-SDS peak no. for complementary fragment
1	Hole HC 1–102 Hole HC 1–101 Hole HC 1–109	11,109 10,992 12,106	11,108 10,992 12,105	HIC pre-peaks 2, 3, 4, 5, 6 & post-peak 2 Post-peaks 5, 6 Pre-peak 4	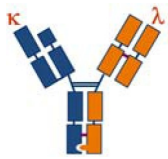	**11**
1′	Knob HC 1–99 Knob HC 1–103 Knob HC 1–106 Knob HC 1–107	11,019 11,403 11,778 11,943	11,019 11,402 11,778 11,942	All HIC fractions HIC pre-peaks 4, 5, 6 HIC pre-peaks 4, 5 HIC pre-peaks 4, 5		
2	κ LC 2–218	23,971	23,969	HIC pre-peaks 7, 6		**10**
3	κ LC + Cys	24,304	24,304	All HIC fractions		
3′	λ LC + Cys	23,041	23041	HIC pre-peaks 5, 6	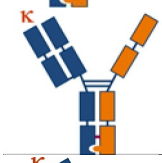	
4	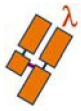 Fab 2 fragment (λ LC knob HC 1–141, 143, 145)	38,370 38,558 38,702	38,370 38,558 38,701	HIC pre-peaks 4, 5, 3 & post-peak 2	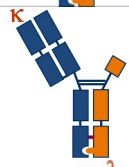	**9**
5	Fab 1 (hole ½Ab)	48,738 48,499 48,256 48,371 48,353	48,737 48,499 48,256 48,371 48,352	HIC pre-peaks 7, 6		**8′**
6	Fab 2 (knob ½Ab)	47,875 47,208 47,637	47,873 47,206 47,639	HIC pre-peaks 4, 5 & post-peak 2		**8**
7	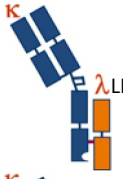 LHL mispair	97,908 97,891 (Su)	97,906 97,890	HIC pre-peak 5 HIC pre-peak 4	**NA** (Only impacted by cell culture condition; no complementary)	**NA**
8	Missing Fab 2 (LHF)	101,903 102,207 101,537	101,905 102,208 101,537	HIC pre-peaks 6, 3 & post-peak 2		**6**
8′	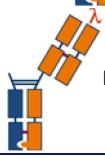 IgG missing Fab 1 (LHF)	101,042 100,675	101,040 100,673	HIC pre-peaks 2, 3, 4 & post-peak 2		**5**

(*Continued*)

Table 1. (Continued).

nrCE-SDS peak no.	Fragment	Mass (Da) Theo	Mass (Da) Detect	HIC enrichment	Complementary fragment	CE-SDS peak no. for complementary fragment
9	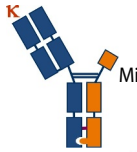 Missing λ LC knob HC 1–141, 143, 145	111,041 110,853 110,709	ND (by LCMS)	HIC pre-peak 5 & post-peak 2		**4**
10	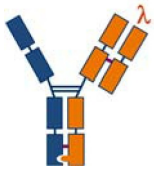 HHL (missing κ LC)	125,209	125,212	Enriched by partial reduction		**3**
		125,209	ND	ND	κ LC 2–218	**2**
	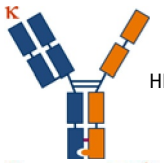 HHL (missing λ LC)	126,472	126477	Enriched by partial reduction		**3′**
11	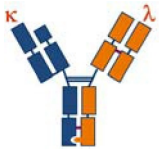 Missing hole HC 1–102 Missing hole HC 1–101 Missing hole HC 1–109	138,302	ND (by LCMS)	HIC pre-peaks 2, 3, 4, 5, 6 & post-peak 2	Hole HC 1–102	**1**
		138,419 137,305		Post-peaks 5, 6 Pre-peak 4	Hole HC 1–101 Hole HC 1–109	
	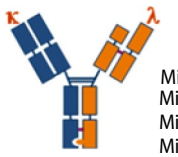 Missing knob HC 1–99 Missing knob HC 1–100 Missing knob HC 1–110 Missing knob HC 1–126	138,392	138,390	HIC post-peaks 5, 6	Knob HC 1–99	**1′**
		138,299 136,980 135,405	138,297 136,980 135,408	HIC pre-peaks 3, 4 HIC pre-peaks 5, 6 HIC pre-peak 3	Knob HC 1–100 Knob HC 1–110 Knob HC 1–126	
Monomer	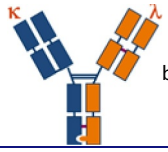 bsAb-A	149,393	149,395	HIC main peak	NA	**NA**

½Ab, half-antibody; LHF, large hinge fragment; NA, not applicable; ND, not determined.

Detection of the clipped but disulfide-linked fragments by LCMS subunit analysis

As described previously, RPLC UV profiles of the crystallizable fragment (Fc) domain and two antigen-binding fragment (Fab) subunits did not show differences in fragments among the three lots of heat-stressed samples because subunits that were clipped but still linked by disulfide would coelute with the main subunit species in RPLC. However, there should be one or multiple 18-Da mass increases in the clipped but disulfide-linked species due to hydrolysis of one or more amide bonds. At the intact antibody level, low numbers of variants with an 18-Da mass shift would not be easily observable in the deconvoluted mass spectrum due to the large size (~150 kDa) and heterogeneity of the antibody. However, mass analysis of antibody subunits results in better resolution and mass accuracy and reduced heterogeneity of each subunit, and therefore should be amenable to detecting the clipped variants in the deconvoluted mass spectra. Furthermore, localization of the clipping region to the Fc subunit or the two Fab subunits would be possible.

The deconvoluted mass spectra from the Fc of drug substance lots A–C that were heat stressed at 40°C for 3 months and the nonstressed control are shown in Figure 6. In comparison with the Fc of the nonstressed control (Figure 6(d)), the Fc from the heat-stressed samples (Figure 6(a-c)) had a noticeable number of variants with one or more mass additions of ~18 Da due to clipping, and these variants were more numerous in lots A and B than in lot C.

To further verify the presence of clipping, sequential digestion using IgdE and peptide N-glycosidase F(PNGase F) was performed, and digests were analyzed by LCMS (Figure6(a-d)). Removal of HC N-glycosylation reduced the complexity of the

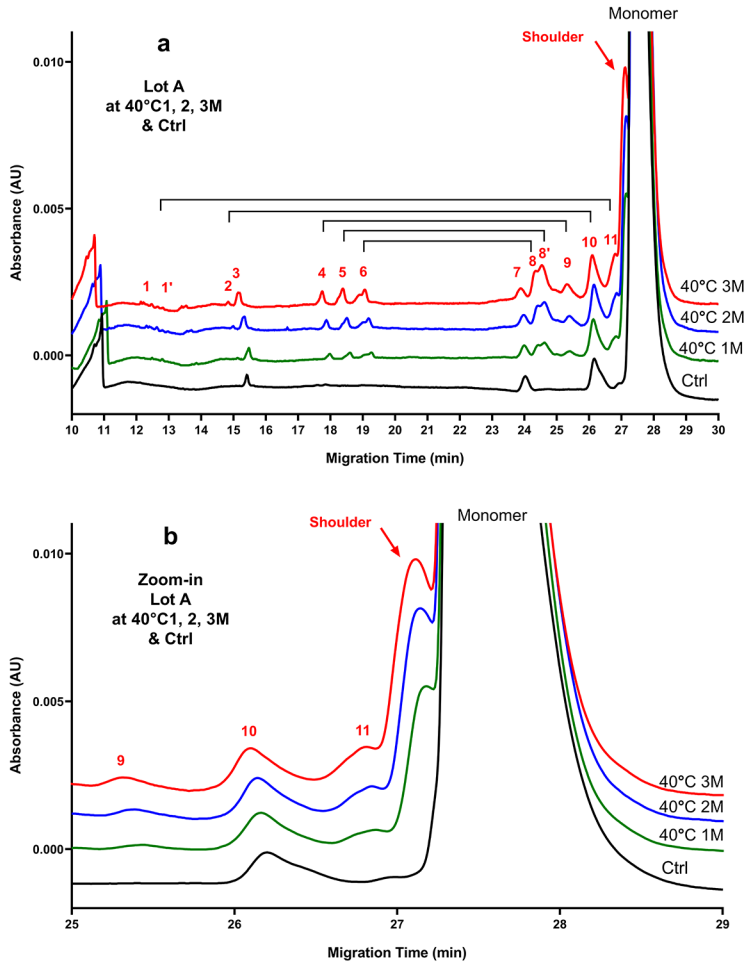

Figure 3. CE-SDS profiles of bsAb-A nonstressed control and lot A heat stressed at 40°C for 1, 2, and 3 months. (a) Electropherogram at full migration time. Horizontal brackets indicate correlations between the N-terminal fragments and their respective C-terminal complementary fragments. (b) Enlarged portion of the electropherogram around the shoulder peak and the main peak.

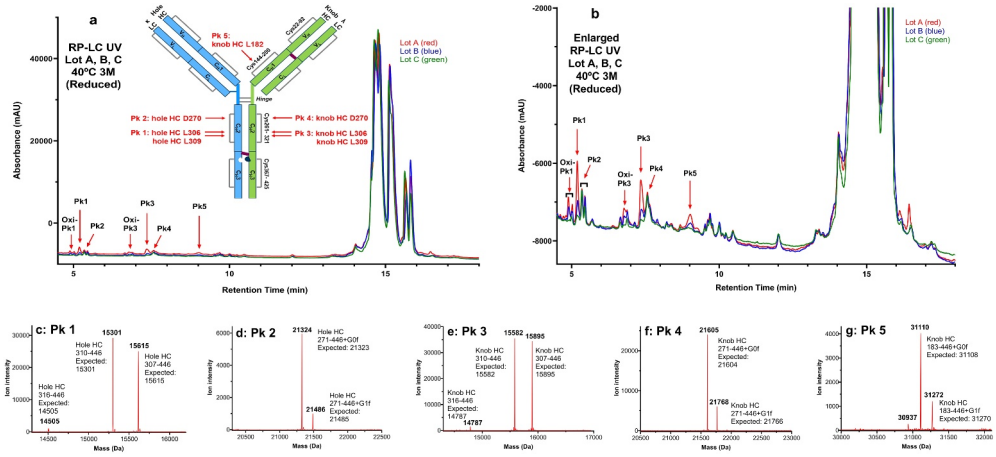

Figure 4. RPLC UV profiles of denatured and reduced bsAb-A drug substance lots heat stressed at 40°C for 3 months and deconvoluted mass spectra of reduced C_H2 and C_H1 fragments. (a) RPLC UV profiles of denatured and reduced bsAb-A heat stressed at 40°C for 3 months; (b) enlargement of RPLC UV profiles of denatured and reduced bsAb-A heat stressed at 40°C for 3 months; (c–g) deconvoluted mass spectra of C_H2 and C_H1 clipped reduced fragments from peak 1 to peak 5, respectively.

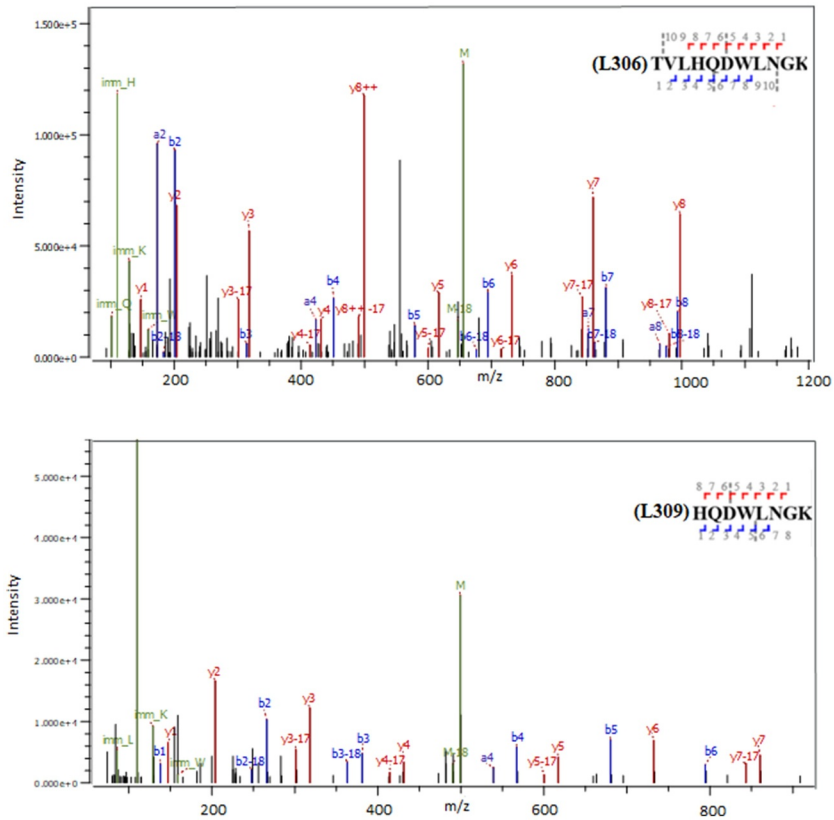

Figure 5. MS/MS of peptides (I)TVLHQDWLNGK resulting from C_H2 clipping at L306 (a) and (L)HQDWLNGK resulting from C_H2 clipping at L309 (b).

deconvoluted mass spectra of Fc, and the data from the deglycosylated Fc further confirmed that Fc clipping increased in the heat-stressed samples, especially in lots A and B.

The clipped but disulfide-linked Fc with one or more ~18-Da mass increases could easily be mistaken as oxidized Fc (+16 Da), due to the similar mass increase, especially by intact mass analysis and if both modifications were present. To resolve this ambiguity, we demonstrated that the oxidized Fc was well resolved from the Fc main peak in RPLC, and the mass was consistent with the theoretical masses of oxidized Fc (Figure 7).

Clipping in the two Fab regions was also examined, and results from lot A drug substance stressed at 40°C for 3 months and nonstressed control are shown as examples in Figure 8. Compared with Fab 2 (the Fab of the knob half-antibody) in the nonstressed control (Figure 8(a')), slightly increased

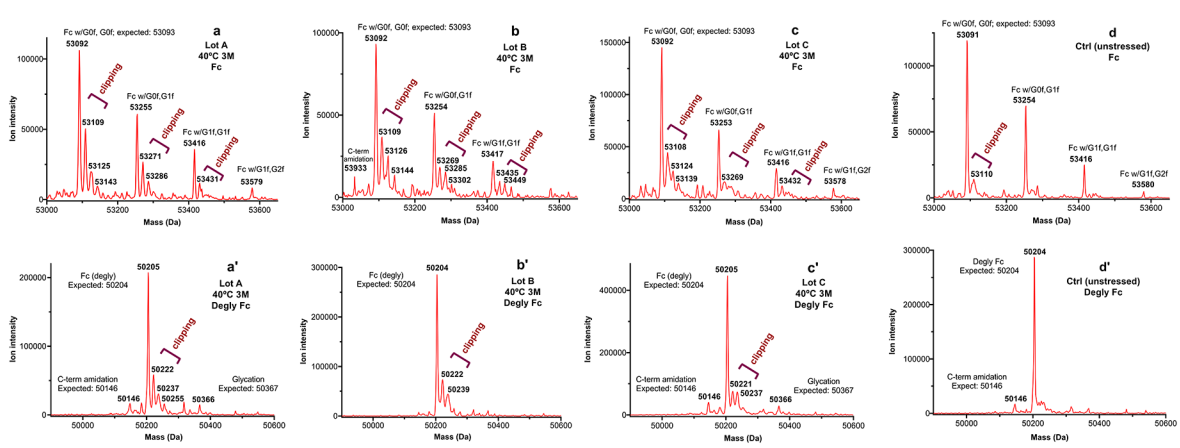

Figure 6. Deconvoluted mass spectra of Fc (top) and deglycosylated Fc (bottom) from 40°C 3-month heat-stressed drug substances of Lot A (a and a'), Lot B (b and b'), Lot C (c and c'), and unstressed control material (d and d').

Table 2. Sequences in the vicinity of CH2 cleavage sites L306 and L309.

EU no.	301	302	303	304	305	306	307	308	309	310	311	312	313	314	315	316	317
IgG1	**R**	**V**	**V**	**S**	**V**	**L**	**T**	**V**	**L**	**H**	**Q**	**D**	**W**	**L**	**N**	**G**	**K**
IgG2	**R**	**V**	**V**	**S**	**V**	**L**	**T**	**V**	**V**	**H**	**Q**	**D**	**W**	**L**	**N**	**G**	**K**
IgG4	**R**	**V**	**V**	**S**	**V**	**L**	**T**	**V**	**L**	**H**	**Q**	**D**	**W**	**L**	**N**	**G**	**K**

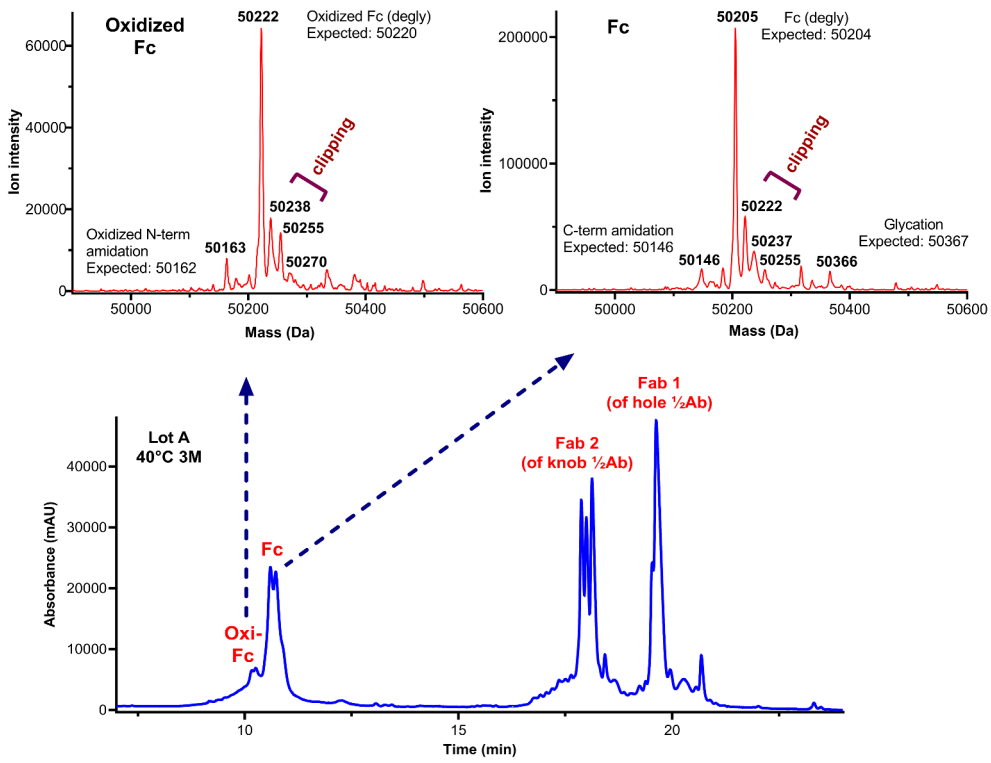

Figure 7. Deconvoluted mass spectra of oxidized Fc and Fc in bsAb-A (top) and RP-LC UV profile of bsAb-A subunits (bottom) of lot A heat stressed at 40°C for 3 months.

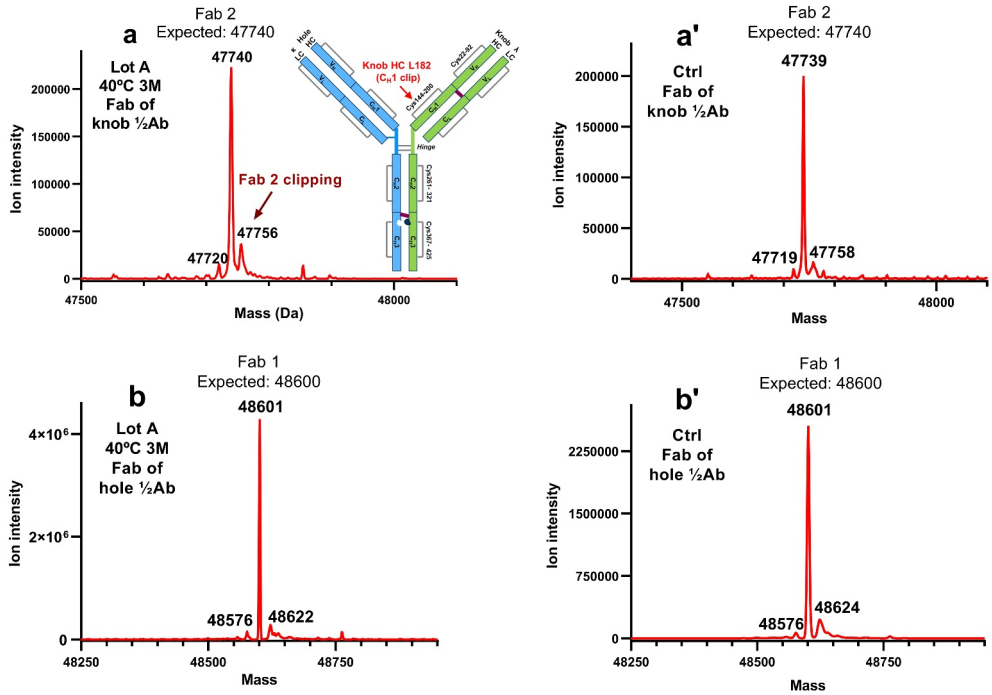

Figure 8. Comparison of deconvoluted mass spectra of Fab2 (a and a′) of the knob half-antibody and Fab1 (b and b′) of the hole half-antibody from bsAb-A lot A drug substance heat stressed at 40°C for 3 months (left) and nonstressed control (right).

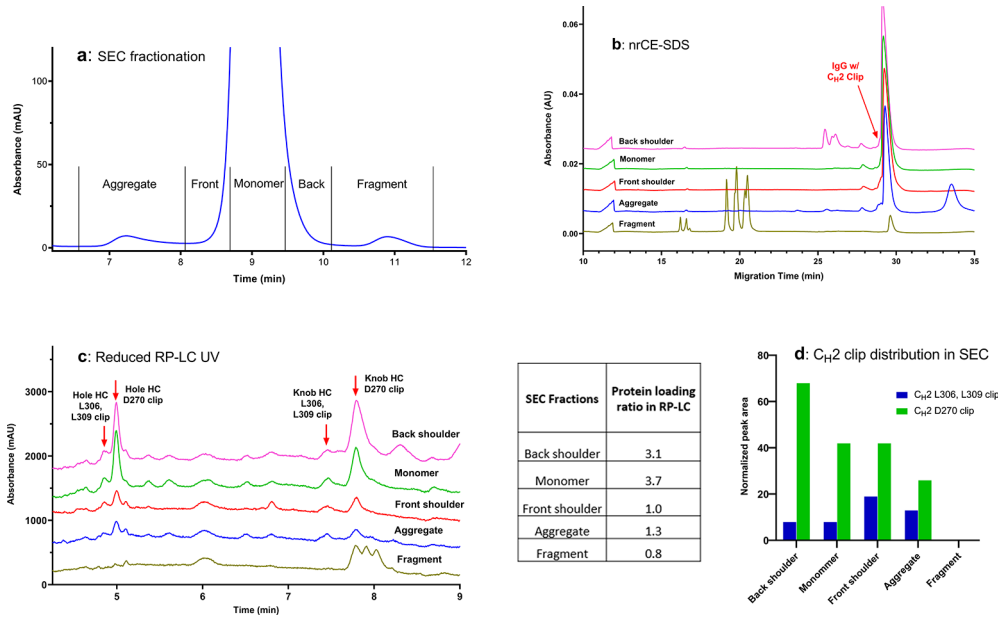

SEC Fractions	Protein loading ratio in RP-LC
Back shoulder	3.1
Monomer	3.7
Front shoulder	1.0
Aggregate	1.3
Fragment	0.8

Figure 9. nrCE-SDS and reduced RPLC UV overlay of SEC fractions from bsAb-A heat stressed at 40°C for 1 month and distribution of C_H2 L306, L309 clipping and D270 clipping in SEC fractions. (a) SEC chromatogram; (b) nrCE-SDS of SEC fractions; (c) reduced RPLC UV of SEC fractions; (d) distribution of C_H2 L306, L309 clipping and D270 clipping in SEC fractions.

clipping was observed in Fab 2 in the heat-stressed lot A drug substance (Figure 8(a')), consistent with the low-level knob HC C_H1 fragment detected by reduced RP-LCMS analysis (peak 5; Figure 4) and Figure 4 insert). In comparison, clipping in Fab 1 (the Fab of the hole half-antibody) was minimal and remained unchanged between the nonstressed control and the heat-stressed lot A drug substances (Figure 8(b,b')).

In summary, fragments linked by an intrachain disulfide bond in heat-stressed bsAb-A samples were mostly due to clipping in the C_H2 domain in the Fc region, and only small amounts of clipping were observed in the C_H1 domain of the knob half-antibody. Different levels of C_H2 clipping at L306 and L309 among the three lots of stability samples (lots A–C) are likely to be the main contributors to the trend observed in the CE-SDS shoulder peak.

Distribution of bsAb-A C_H2 clipping in SEC fractions

To determine whether bsAb-A fragments from C_H2 clipping at L306, L309, and D270 could be isolated and enriched by SEC, the SEC fractions collected from lot D bsAb-A drug substance that had been heat stressed at 40°C for 1 month were analyzed by reduced RP-LCMS and nrCE-SDS (Figure 9). Different amounts of total proteins of SEC fractions were loaded onto the RPLC column; normalization factors are listed in Figure 9. After taking into account the sample loading differences, the adjusted peak areas of fragments from C_H2 clipping at L306, L309, and D270 in the SEC fractions were plotted (Figure 9(d)). Overall, C_H2 fragments clipped at L306, L309, and D270 were distributed across all SEC fractions except the fragment fraction; the SEC fragment was identified as small hinge fragments (Fabs) containing no Fc.

The results of this study suggest that C_H2 clipping is present in molecules with different hydrodynamic volumes, and the C_H2 clipped molecules do not have sufficiently different hydrodynamic volumes to be resolved from the unclipped molecules and thus cannot be isolated or enriched by SEC. This finding was also confirmed by SEC fraction studies of several other in-house IgG1 and IgG4 molecules in which detectible L306, L309, or D270 clipping by reduced RPLC analysis were observed (data not shown).

C_H2 cleavage at L306 and L309 in IgGs

The two major C_H2 cleavage sites (L306 and L309) that contribute to the CE-SDS shoulder peak are highly conserved amino acids across IgG1 and IgG4s and partially conserved in IgG2s at L306 (Table 2). To generate platform knowledge of C_H2 clipping at L306 and L309 (valine 309 in IgG2) conserved sites, we performed peptide mapping analysis of 13 different IgG1, IgG2, and IgG4 antibody samples that were heat stressed at 40°C for 2 or 3 months. Within the IgG1 subclass, the wild type, the IgG1 with Fc triple mutations L234F, L235E, and P331S (TM)[20] and with YTE mutations (M252Y, S254T, and T256E)[21] were included. Within IgG4, the wild type and the IgG4 with hinge mutations (CPSC mutated to CSSC) are included. Peptide mapping data showed detectable cleavages at L306 and L309 and neighboring sites in the vicinity of these two sites in all IgG1 and IgG4 heat-stressed samples tested in this study.

Similar to IgG1 and IgG4, the IgG2 molecule that was heat stressed at 40°C for 3 months had detectable cleavage at L306 as well as the neighboring D312 site by peptide mapping; unlike the cleavage at L309 in IgG1 and IgG4, there was no detectable cleavage at V309 in the IgG2 molecule. However, further work with more IgG2 molecules is needed to confirm whether the current observation of IgG2 C_H2 cleavage sites is widely representative of this subclass.

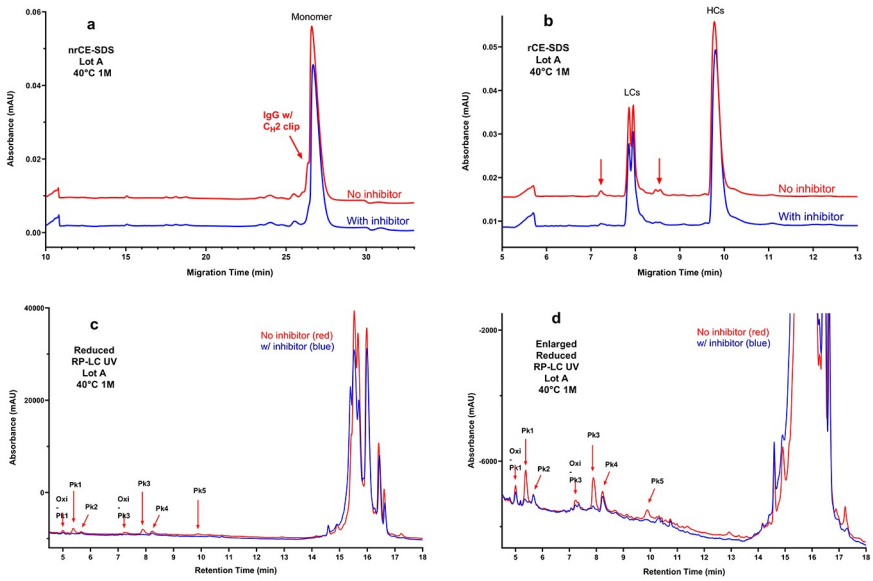

Figure 10. Overlays of nrCE-SDS (a), rCE-SDS (b), reduced RPLC UV (c) and enlarged view of reduced RPLC UV (d) of bsAb lot A drug substance heat stressed at 40°C for 1 month and incubated with and without protease inhibitor.

In summary, we observed detectable C_H2 cleavages at L306 and L309 in all IgG1 and IgG4 molecules studied, including the respective wild types, IgG1s with TM or YTE mutations, and IgG4s with hinge mutations. The C_H2 cleavage at L306 was also observed in the only IgG2 molecule studied.

C_H1 and C_H2 clippings inhibited by protease inhibitors

Fragments can be generated as a result of either a spontaneous or an enzymatic reaction. Liu et al.[18] have reported that fragments from direct hydrolysis at antibody labile spots, such as the hinge region and the C_H2-C_H3 interface, are common for mAbs at high temperature. Other studies[9] have also shown that several sites in the hinge region and the C_H2-C_H3 interfaces can be prone to enzymatic cleavage after brief exposure to low pH. The LambdaFabSelect elution in bsAb-A manufacturing or the protein A elution in mAb manufacturing, as well as low pH hold treatments for viral inactivation in both manufacturing processes, provide the possibility for hinge and C_H2-C_H3 cleavages by host cell proteases. Similar to direct hydrolysis, protease cleavage propensities increase with heat stress. To investigate the potential proteolytic activity as a root cause for the observed C_H2 clipping at L306, L309, and D270 and the C_H1 clipping at L182 in bsAb-A, a protease inhibitor cocktail was spiked into bsAb-A drug substance lot A and incubated at 40°C for 1 month, along with the drug substance with no spiked protease inhibitors as a control. The samples were subsequently analyzed by nrCE-SDS, rCE-SDS, and reduced RP-LCMS; overlays from the three assays are shown in Figure 10.

For the sample incubated with protease inhibitors, the shoulder peak in nrCE-SDS (Figure 10(a)) and the two associated peaks in rCE-SDS (Figure 10(b)) were substantially decreased. Consistent with the CE-SDS results, reduced RP-LCMS data confirmed that the C_H2 clipping at L306 and L309 (peaks 1 and 3), their oxidized forms, and the C_H1 clipping on the knob HC at L182 (peak 5) was greatly reduced (Figure 10(c, d)). These data demonstrate that protease cleavages are most likely to account for the majority of the clipping observed at these sites in bsAb-A. These fragment peaks in CE-SDS can be significantly reduced by inhibiting protease activities. The oxidized forms of C_H2 clipping at L306 and L309 observed in the RP-LC UV profile (Oxi-Pk 1 and Oxi-Pk 3; Figure 10(c,d) coeluted with another fragment, and therefore the UV intensity of these two peaks decreased only moderately in the sample incubated with protease inhibitor. MS data, however, showed that the oxidized forms of peaks 1 and 3 were minimized in both peaks with a 10-fold decrease in the observed MS signal.

C_H2 clipping at D270 on both HCs (peaks 2 and 4; Figure 10(c, d), in contrast, were not significantly affected by incubation with protease inhibitors, indicating that the mechanism of the observed D270 clipping in C_H2 was likely to be direct hydrolysis under heat stress, with only minimal, if any, contributions from proteolysis.

In both the protease-inhibiting study and the earlier heat-stress study, there was a clear correlation between the shoulder peak in nrCE-SDS, the two associated peaks in rCE-SDS, and the C_H2 clipping at HC L306, L309. Taken together, these data provide further support for the identity of the species comprising the shoulder peak observed in nrCE-SDS.

Discussion

Fragments generated from clipping but still linked by intrachain disulfide bonds are not uncommon, especially in the C_H2 domain. One example is the C_H2 DP clipping at D270, which is commonly observed in IgGs and bsAbs[2,8,11,15,17,18] and has been observed in nonstressed materials. These clipped but disulfide-linked fragments are usually identified through the detection of the reduced forms by reduced RP-LCMS, rCE-SDS, and peptide mapping, as enrichment of the nonreduced forms of these clipped species is challenging. The nonreduced form coelutes with intact IgGs in RPLC[15] and is distributed broadly in SEC fractions (Figure 9) and HIC fractions (data not shown), and we have also observed C_H2 DP clipping distributed across ion-exchange chromatography (IEC) fractions at comparable levels (Supplementary Figure S4). Considering the challenges in directly detecting or enriching the nonreduced form of the C_H2 clipped fragments, it is not surprising that this species in nrCE-SDS has not been identified or reported previously and has been hypothesized to comigrate with intact IgG in nrCE-SDS.[15]

Our findings reveal that mAbs and bsAbs containing disulfide-linked fragments from C_H2 clipping can be partially resolved as the front shoulder of the main peak in nrCE-SDS. This front shoulder peak from C_H2 clipping can also be resolved from the previously reported nrCE-SDS shoulder peak resulting from IgG missing HC N-terminal ~100 amino acid species, as demonstrated in the nrCE-SDS study of bsAb-A described here.

To our knowledge, this is the first report demonstrating that clippings that are within the C_H2 domain but are still covalently linked by an intrachain disulfide bond can be resolved by nrCE-SDS. Contrary to previous reports speculating that these species comigrate with intact IgG in nrCE-SDS, we observed that they migrated earlier as a shoulder peak when present in detectable amounts. The observation that the C_H2 clipped but disulfide-linked fragment migrated slightly earlier than the intact IgG has at least three possible explanations: 1) IgG with disulfide linkages in nonreducing gel may not be stretched to be completely linear; 2) C_H2 clipping may break some C_H2-C_H2 interactions and allow the molecule more access to SDS binding, resulting in higher total negative charges; and 3) with its mass similar to intact IgG (+18 Da), the C_H2 clipped but disulfide-linked fragment has a smaller mass-to-charge ratio and migrates earlier than intact IgG in nrCE-SDS.

Since the lower hinge/C_H2 interface and C_H2 domain are among the most cleaved regions in IgG1, it is important to understand their presence in IgG subclasses (IgG1, IgG4, and IgG2) and their separation in nrCE-SDS, rCE-SDS, SEC, HIC, and IEC. Identifying these clipping sites and the root causes of these clippings could reveal additional degradation pathways. Our study suggests the amount of nrCE-SDS shoulder peak in bsAb or mAb stability samples could be directly linked to the level of the host cell protease that cleaves at C_H2 L306, L309, and to a lesser extent at C_H1 L182. A relatively higher level of this nrCE-SDS shoulder peak would require optimization of the cell culture and purification processes to remove host cell protease and reduce protease-related fragments, which could potentially improve manufacturing control of product quality. Our findings may help manufacturers of therapeutic antibodies with their investigations, in particular, product characterization, formulation stability, and stability comparability studies.

Materials and methods

Reagents and materials

Engineered bsAb-A was produced from a Chinese hamster ovary host cell line by AstraZeneca. Sodium sulfate, sodium acetate N-ethylmaleimide, sodium phosphate dibasic, sodium phosphate monobasic monohydrate, sodium chloride, formic acid, trifluoroacetic acid (TFA), 2-mercaptoethanol, and protease inhibitor cocktail (Catalog number P8465) were obtained from Sigma. Urea (OmniPur), water (OmniSolv, HPLC and spectrophotometry grade), acetonitrile (OmniSolv, HPLC and spectrophotometry grade), and isopropyl alcohol (OmniSolv, HPLC and spectrophotometry grade) were obtained from EMD Serono. Trypsin (Catalog number V5280) and PNGase F (Catalog number V483A) were obtained from Promega. Dithiothreitol (no-weight format) was obtained from Pierce Protein Biology. FabALACTICA (IgdE) was from Genovis.

HIC

A Thermo MabPac HIC-10, 5 µm, 1000 Å column (4.6 × 250 mm) was used for HIC chromatography. Mobile phase A consisted of 50 mM sodium phosphate, 1.0 M sodium sulfate, pH 6.5, and mobile phase B consisted of 50 mM sodium phosphate, pH 6.5. Samples of bsAb-A were diluted to 1 mg/mL in HPLC water, and 50 µL was injected onto the HIC column. The column temperature was set at 30°C. The sample was eluted in a gradient of 20% to 100% mobile phase B over 25 minutes at a flow rate of 1 mL/min. Eluted protein was detected by UV absorbance at a wavelength of 280 nm.

UV RP-LCMS

For intact RP-LCMS analysis, the sample was diluted to 1 mg/mL in water. For reduced RP-LCMS analysis, the sample was diluted to 1 mg/mL in 4 M guanidine hydrochloride, 65 mM tris-(hydroxymethyl)aminomethane (Tris) buffer, 0.5 mM ethylenediaminetetraacetic acid at pH 7.6 and reduced in 10 mM dithiothreitol at 37°C for 30 min. Two microliters of each sample were injected onto a Waters BioResolve RP mAb polyphenyl column (2.1 × 150 mm, 2.7 µm, 450 Å) heated at 75°C. Mobile phase A consisted of 0.07% trifluoroacetic acid (TFA), 0.1% formic acid (FA) in water, and mobile phase B consisted of 0.07% TFA, 0.1% FA in acetonitrile. A gradient of 30% to 36% mobile phase B was run from 2 to 23 min at a flow rate of 0.2 mL/min. The eluted protein was detected by UV absorbance at a wavelength of 280 nm.

Each sample was diluted to 1 mg/mL in water. Two microliters of each sample were injected onto a Waters BioResolve RP mAb polyphenyl column (2.1 × 150 mm, 2.7 µm, 450 Å) heated at 75°C. Mobile phase A consisted of 0.07% TFA, 0.1% FA in water, and mobile phase B consisted of 0.07% TFA, 0.1% FA in

acetonitrile. A gradient of 30% to 36% mobile phase B was run from 2 to 23 min at a flow rate of 0.2 mL/min. The eluted protein was detected by UV absorbance at a wavelength of 280 nm.

CE-SDS analysis

Samples were denatured in a prepared sample buffer with 100 mM sodium phosphate and 4% SDS at pH 6.5. Samples were diluted to 1.0 mg/mL in 50% (vol/vol) sample buffer, 5% (vol/vol) N-ethylmaleimide (300 mM stock), and water for nonreduced analysis or 5% (vol/vol) 2-mercaptoethanol stock solution for reduced analysis. Samples were then incubated on a heating block at 65°C for 10 min. Following heating, samples were spun at 13,200 rpm to cool and collect the condensate. Samples were then loaded into microvials and placed in a SCIEX PA 800 Plus CE system. The autosampler was set to 15°C for sample storage before testing. For the nonreduced method, the capillary length was 30.2 cm with an effective separation length of 20.2 cm and a run time of 40 min. For the reduced method, the effective separation length was 10 cm, and the run time was 20 min. Both separation methods used the same conditions with injection voltage at 5 kV and separation voltage at 15 kV. Capillary temperature was 25°C. The photodiode array detector wavelength was 220 nm. Data were collected through 32 Karat Software and then exported to Empower for data analysis.

Peptide mapping

Samples were denatured and reduced at 37°C for 30 min with buffer (7.2 M guanidine hydrochloride, 0.1 mM ethylenediaminetetraacetic acid, 90 mM Tris, 30 mM dithiothreitol at pH 7.4). Samples were then alkylated by 2-iodoacetamide (at a final concentration of 70 mM) at room temperature in the dark for 30 min. This was followed by microdialysis to the buffer comprising 6 M urea and 150 mM Tris, pH 7.6. Samples were then diluted to 0.45 mg/mL with 100 mM Tris, pH 7.5; trypsin was added at a mass ratio of 1:12 (enzyme:protein); and the mixture was incubated at 37°C for 4 h and then quenched with TFA solution. A Fusion mass spectrometer (Thermo Fisher Scientific) connected with an Acquity ultraperformance liquid chromatograph (UPLC) (Waters) was used for peptide map analysis. An Acquity UPLC BEH300 C18 column (1.7 µm, 2.1 × 150 mm; Waters) was used for separation. The column temperature was held at 55°C. Mobile phase A was 0.02% TFA in water, and mobile phase B was 0.02% TFA in acetonitrile. Digested peptides were eluted from the column by gradient, and the chromatographic profile was monitored by UV absorbance at a wavelength of 220 nm.

Subunit IgdE digestion

For IgdE digestion, the sample was first diluted to 1 mg/mL in 100 mM phosphate buffer at pH 7.0. The reconstituted IgdE solution was then added at a ratio of 1 unit per µg of protein, and the mixture was incubated at 37°C for 16–18 h.

PNGase F digestion

For deglycosylation, samples were diluted to 1 mg/mL in Tris buffer (pH 7.5); PNGase F was diluted 1:1 in water. Diluted PNGase F was added to the sample at a ratio of 0.05 unit per µg of protein, and the mixture was incubated at 37°C overnight.

SEC analysis

SEC analysis was performed by loading 80 µg of each bsAb-A sample onto a BEH SEC 200 Å, 1.7-µm, 4.6 × 150–mm column at ambient column temperature. The sample was eluted isocratically with a mobile phase composed of 0.1 M sodium phosphate, 0.1 M sodium sulfate, and 0.05% sodium azide, pH 6.8, at a flow rate of 0.2 mL/min over 15 minutes. Eluted protein was detected by UV absorbance at a wavelength of 280 nm.

Abbreviations

CE-SDS	capillary electrophoresis sodium dodecyl sulfate
nrCE-SDS	nonreduced capillary electrophoresis sodium dodecyl sulfate
rCE-SDS	reduced capillary electrophoresis sodium dodecyl sulfate
RP-UPLC	reverse phase ultra-performance liquid chromatography
RP-LCMS	reverse phase liquid chromatography mass spectrometry
mAb	monoclonal antibody
SEC	size exclusion chromatography
CDR	complementarity-determining region
MS/MS	tandem mass spectrometry
LCMS	liquid chromatography mass spectrometry
HIC	hydrophobic interaction chromatography
bsAb	bispecific antibody
MS	mass spectrometry
½Ab	half-antibody
Fab	antigen-binding fragment
Fc	crystallizable fragment
IgG	immunoglobulin
LC	light chain
HC	heavy chain
IEC	ion exchange chromatography
TFA	trifluoroacetic acid
UPLC	ultra-performance liquid chromatography

Acknowledgments

The authors thank Jared Delmar and Rupesh Bommana for sharing their heat-stressed IgG samples and related reduced RP-LCMS and peptide mapping results. Editorial support was provided by Deborah Shuman of AstraZeneca.

Disclosure statement

All authors are employees of AstraZeneca and may hold stock interests in the company.

Funding

The author(s) reported there is no funding associated with the work featured in this article.

ORCID

Mingyan Cao http://orcid.org/0000-0001-5277-4962

References

1. Dada OO, Rao R, Jones N, Jaya N, Salas-Solano O. Comparison of SEC and CE-SDS methods for monitoring hinge fragmentation in IgG1 monoclonal antibodies. J Pharm Biomed Anal. 2017;145:91–97. doi:10.1016/j.jpba.2017.06.006. PMID: 28654781.
2. Vlasak J, Ionescu R. Fragmentation of monoclonal antibodies. mAbs. 2011;3(3):253–63. doi:10.4161/mabs.3.3.15608. PMID: 21487244.
3. Rustandi RR, Washabaugh MW, Wang Y. Applications of CE SDS gel in development of biopharmaceutical antibody-based products. Electrophoresis. 2008;29(17):3612–20. doi:10.1002/elps.200700958. PMID: 18803223.
4. Ouellette D, Alessandri L, Piparia R, Aikhoje A, Chin A, Radziejewski C, Correia I. Elevated cleavage of human immunoglobulin gamma molecules containing a lambda light chain mediated by iron and histidine. Anal Biochem. 2009;389(2):107–17. doi:10.1016/j.ab.2009.03.027. PMID: 19318085.
5. Wagner E, Colas O, Chenu S, Goyon A, Murisier A, Cianferani S, François Y, Fekete S, Guillarme D, D'Atri V, et al. Determination of size variants by CE-SDS for approved therapeutic antibodies: key implications of subclasses and light chain specificities. J Pharm Biomed Anal. 2020;184:113166. doi:10.1016/j.jpba.2020.113166. PMID: 32113118.
6. O'Connor E, Aspelund M, Bartnik F, Berge M, Coughlin K, Kambarami M, Spencer D, Yan H, Wang W. Monoclonal antibody fragment removal mediated by mixed mode resins. J Chromatogr A. 2017;1499:65–77. doi:10.1016/j.chroma.2017.03.063. PMID: 28389094.
7. Rouby G, Tran NT, Leblanc Y, Taverna M, Bihoreau N. Investigation of monoclonal antibody dimers in a final formulated drug by separation techniques coupled to native mass spectrometry. mAbs. 2020;12(1):e1781743. doi:10.1080/19420862.2020.1781743. PMID: 32633190.
8. Faid V, Leblanc Y, Bihoreau N, Chevreux G. Middle-up analysis of monoclonal antibodies after combined IgdE and IdeS hinge proteolysis: investigation of free sulfhydryls. J Pharm Biomed Anal. 2018;149:541–46. doi:10.1016/j.jpba.2017.11.046. PMID: 29179100.
9. Gao SX, Zhang Y, Stansberry-Perkins K, Buko A, Bai S, Nguyen V, Brader ML. Fragmentation of a highly purified monoclonal antibody attributed to residual CHO cell protease activity. Biotechnol Bioeng. 2011;108(4):977–82. doi:10.1002/bit.22982. PMID: 21404269.
10. Gaza-Bulseco G, Liu H. Fragmentation of a recombinant monoclonal antibody at various pH. Pharm Res. 2008;25(8):1881–90. doi:10.1007/s11095-008-9606-3. PMID: 18473123.
11. Lu C, Liu D, Liu H, Motchnik P. Characterization of monoclonal antibody size variants containing extra light chains. mAbs. 2013;5(1):102–13. doi:10.4161/mabs.22965. PMID: 23255003.
12. Kubota K, Kobayashi N, Yabuta M, Ohara M, Naito T, Kubo T, Otsuka K. Identification and characterization of a thermally cleaved fragment of monoclonal antibody-A detected by sodium dodecyl sulfate-capillary gel electrophoresis. J Pharm Biomed Anal. 2017;140:98–104. doi:10.1016/j.jpba.2017.03.027. PMID: 28346883.
13. Li W, Yang B, Zhou D, Xu J, Li W, Suen WC. Identification and characterization of monoclonal antibody fragments cleaved at the complementarity determining region using orthogonal analytical methods. J Chromatogr B Analyt Technol Biomed Life Sci. 2017;1048:121–29. doi:10.1016/j.jchromb.2017.02.019. PMID: 28242491.
14. Kaschak T, Boyd D, Yan B. Characterization of glycation in an IgG1 by capillary electrophoresis sodium dodecyl sulfate and mass spectrometry. Anal Biochem. 2011;417(2):256–63. doi:10.1016/j.ab.2011.06.024. PMID: 21756870.
15. Wang WH, Cheung-Lau J, Chen Y, Lewis M, Tang QM. Specific and high-resolution identification of monoclonal antibody fragments detected by capillary electrophoresis-sodium dodecyl sulfate using reversed-phase HPLC with top-down mass spectrometry analysis. mAbs. 2019;11(7):1233–44. doi:10.1080/19420862.2019.1646554. PMID: 31348730.
16. Tous GI, Wei Z, Feng J, Bilbulian S, Bowen S, Smith J, Strouse R, McGeehan P, Casas-Finet J, Schenerman MA. Characterization of a novel modification to monoclonal antibodies: thioether cross-link of heavy and light chains. Anal Chem. 2005;77(9):2675–82. doi:10.1021/ac0500582. PMID: 15859580.
17. Liu H, Gaza-Bulseco G, Lundell E. Assessment of antibody fragmentation by reversed-phase liquid chromatography and mass spectrometry. J Chromatogr B Analyt Technol Biomed Life Sci. 2008;876(1):13–23. doi:10.1016/j.jchromb.2008.10.015. PMID: 18993120.
18. Liu H, Gaza-Bulseco G, Faldu D, Chumsae C, Sun J. Heterogeneity of monoclonal antibodies. J Pharm Sci. 2008;97:2426–47. doi:10.1002/jps.21180. PMID: 17828757.
19. Cao M, Parthemore C, Jiao Y, Korman S, Aspelund M, Hunter A, Kilby G, Chen X. Characterization and monitoring of a novel light-heavy-light chain mispair in a therapeutic bispecific antibody. J Pharm Sci. 2021;110(8):2904–15. doi:10.1016/j.xphs.2021.04.010. PMID: 33894207.
20. Oganesyan V, Gao C, Shirinian L, Wu H, Dall'Acqua WF. Structural characterization of a human Fc fragment engineered for lack of effector functions. Acta Crystallogr D Biol Crystallogr. 2008;64(6):700–04. doi:10.1107/s0907444908007877. PMID: 18560159.
21. Oganesyan V, Damschroder MM, Woods RM, Cook KE, Wu H, Dall'acqua WF. Structural characterization of a human Fc fragment engineered for extended serum half-life. Mol Immunol. 2009;46(8–9):1750–55. doi:10.1016/j.molimm.2009.01.026. PMID: 19250681.